Front. Earth Sci. China 2010, 4(2): 237–252
DOI 10.1007/s11707-010-0002-z

REVIEW ARTICLE

An overview of sensor calibration inter-comparison and applications

Xiaoxiong (Jack) XIONG (✉)[1], Changyong CAO[2], Gyanesh CHANDER[3]

1 NASA Goddard Space Flight Center (GSFC), Sciences Exploration Directorate, Greenbelt, MD 20771, USA
2 NOAA National Environmental Satellite, Data, and Information Service (NESDIS), Office of Research and Applications, Camp Springs, MD 20746, USA
3 SGT, Inc., U.S. Geological Survey (USGS) Earth Resources Observation and Science (EROS) Center, Sioux Falls, SD 57198, USA

Abstract Long-term climate data records (CDR) are often constructed using observations made by multiple Earth observing sensors over a broad range of spectra and a large scale in both time and space. These sensors can be of the same or different types operated on the same or different platforms. They can be developed and built with different technologies and are likely operated over different time spans. It has been known that the uncertainty of climate models and data records depends not only on the calibration quality (accuracy and stability) of individual sensors, but also on their calibration consistency across instruments and platforms. Therefore, sensor calibration inter-comparison and validation have become increasingly demanding and will continue to play an important role for a better understanding of the science product quality. This paper provides an overview of different methodologies, which have been successfully applied for sensor calibration inter-comparison. Specific examples using different sensors, including MODIS, AVHRR, and ETM+, are presented to illustrate the implementation of these methodologies.

Keywords radiometer, MODIS, AVHRR, ETM+, calibration, inter-comparison

1 Introduction

The Earth-observing sensors' calibration accuracy and consistency over time are critical performance parameters, and have a direct impact on the quality of the data products derived from their on-orbit observations. As more and more satellite observations become available to the science and user community, the number of science data products and their applications continue to increase, including the data products used to predicate or understand climate change. The long-term climate data records (CDR) are often constructed using observations made by multiple sensors. These sensors, either of the same or different types, could be operated on the same or different platforms. Even sensors of the same type can be developed and built with different technologies by different instrument vendors and operated over different time spans. Some sensors may have been built without adequate on-board calibration, and have not gone through comprehensive system-level pre-launch characterization, thus cannot firmly establish their calibration traceability and consistently maintain the calibration stability. It is not surprising that cross-sensor calibration inter-comparison has become increasingly important and demanding, in addition to individual calibration accuracies. (Ohring et al., 2008).

In May 1995, a Workshop on Strategies for Calibration and Validation of Global Change and Measurements was organized by the NASA Goddard Space Flight Center (GSFC), on behalf of the Committee on Earth Observation Satellites (CEOS) Working Group on Calibration/Validation (WGCV), the Global Change Observing System (GCOS), and the US Committee on Environment and Natural Resources (CENR). One of the key findings of this workshop addressed the importance of the data set continuity and consistency (Guenther et al., 1997). A similar Workshop on Satellite Instrument Calibration for Measuring Global Climate Change was jointly organized in 2002 by the National Institute of Standards, and Technology (NIST), NOAA, NASA, and National Polar-orbiting Operational Environmental Satellite System (NPOESS) Integrated Program Office (IPO) with focus on identifying the requirements and challenges of measuring small changes associated with long-term global climate

Received September 30, 2009; accepted October 30, 2009

E-mail: Xiaoxiong.Xiong-1@nasa.gov

change (Ohring et al., 2004). A follow-on workshop, Achieving Satellite Instrument Calibration for Climate Change (ASIC[3]), was held in April 2006, with its primary objective set to formulate a national roadmap for a calibration system that will help the remote sensing community to achieve the requirements and meet the challenges (Ohring et al., 2008). Meanwhile, a broad international effort has also been made to use integrated satellite data in support of decision making for different organizations and agencies. For example, the Global Earth Observation System of Systems (GEOSS) is currently being built as an emerging public infrastructure interconnecting a diverse and growing array of instruments and systems for monitoring and forecasting changes in the global environment. This "system of systems", with more than 78 participating national governments plus the European Commission, supports policymakers, resource managers, science researchers and many other experts and decision-makers.

The GEOSS aims to deliver comprehensive "knowledge information products" in a timely manner to meet the needs of its nine "Societal Benefit Areas", of which the most demanding, in terms of accuracy, is climate. To accomplish this vision, starting from a system of disparate systems that are built for a wide range of applications, it requires the establishment of an internationally coordinated operational framework to facilitate interoperability and harmonization. CEOS, the world space agency committee, has taken on the task of being responsible for the space segment of GEOSS. It is recognized that the success of GEOSS critically depends on the interoperability of a diverse system of systems, with data access and data quality assurance being the two key aspects of interoperability. Specifically, the CEOS WGCV has been tasked to develop a data quality assurance strategy for the GEOSS with key guidelines. Several tasks and actions have been initiated to establish calibration consistency and standards across systems, including the establishment of CEOS reference standard test sites[1)] and a traceability chain for primary site data and "best practices" guidance on site characterization and applications. The recent development of a Quality Assurance Framework for Earth Observation (QA4EO) is such an example.

The objective of this paper is to provide an overview of sensor calibration inter-comparison methodologies and their applications. Since not all the Earth-observing sensors have well characterized on-board calibrators, especially in the solar reflective spectral region, the methodologies presented in this paper are based on using well-characterized ground targets, near simultaneous nadir overpasses (SNO), an intermediate transfer sensor, and the Moon. Although the discussions are fairly general, the examples illustrated in this paper will be focused on the filter radiometers and/or imagers, such as MODIS, AVHRR, and ETM+. These sensors are selected largely because their observations have been widely used by the science community. MODIS is a keystone instrument for NASA's Earth Observing System (EOS) mission, currently operated on both the Terra and Aqua spacecrafts launched in December 1999 and May 2002, respectively. Since launch, nearly 40 science data products from MODIS observations have been continuously produced and widely distributed for studies of the Earth's land, ocean, and atmospheric properties, and their short- and long-term changes (Esaias et al., 1998; Justice et al., 1998; Salomonson et al., 2002; King et al., 2003; Parkinson, 2003). The nearly 30 years of AVHRR observations have provided the basis for developing many of the key climate data records (CDR), such as vegetation, aerosols, outgoing long-wave radiation, and land and ocean surface temperatures. However, the quality of the CDR and the credibility of the climate change detection critically depend on the consistency and accuracy of the satellite instrument calibration (Heidinger et al., 2002; Trishchenko et al., 2002; Cao et al., 2005, 2008). From its inception in 1972 to present, the Landsat series of satellites has provided the longest continuous record of satellite-based observations, which have significantly benefited the earth science user community (Goward and Williams, 1997; Cohen and Goward, 2004; Goward et al., 2006). The Landsat data archive at the U.S. Geological Survey (USGS) Earth Resources Observation and Science (EROS) Center holds an unequaled 36-year record of the Earth's surface and is now available at no cost to users via the Internet.

Following a brief sensor overview in Section 2 of this paper, Section 3 provides details on different sensor calibration inter-comparison methodologies, including approaches using the simultaneous nadir overpass (SNO), an intermediate sensor, ground targets, and the Moon. Applications and results from these approaches are illustrated in Section 4. Discussed in Section 5 are key issues critical to calibration inter-comparison quality and major challenges for further improvements. A summary of this paper is provided in Section 6. It is clear that with the increased effort to establish calibration consistency among existing sensors and with the improved design and calibration quality of future sensors, the quality of the long-term climate data records will be significantly improved. The methodologies and examples presented in this paper will continue to serve as references for future sensor inter-comparison studies and applications.

2 Instrument background

To establish and assure the quality of sensor calibration inter-comparison work, including better characterization of calibration differences among sensors and assessment of

1) http://calval.cr.usgs.gov/sites_catalog_map.php

their calibration impact on the derived data products, it is extremely important to have a clear understanding of sensor features or characteristics. For reference purposes, a brief description of MODIS, AVHRR, and ETM+ is provided in the following.

2.1 MODIS

MODIS was developed based on a number of heritage sensors, including AVHRR and ETM+, with improved capabilities and calibration requirements (Barnes and Salomonson, 1993). MODIS data is collected in 36 spectral bands covering wavelengths from 0.41 to 14.4 μm and at 3 spatial resolutions: 250 m (bands 1–2), 500 m (bands 3–7), and 1 km (bands 8–36). It is a cross-track scanning (whisk broom) radiometer via a two-sided scan mirror, making the Earth observations over a scan angle range of ±55° relative to instrument nadir, enabling a complete global coverage of the Earth's surface in less than 2 days. A summary of MODIS key design requirements and primary applications for each spectral band is provided in Table 1. A major improvement of MODIS instrument design over its heritage sensor has been its on-board calibrators (OBC) and their on-orbit calibration and characterization functions. MODIS OBC include a solar diffuser (SD), a solar diffuser stability monitor (SDSM), a blackbody (BB), and a spectro-radiometric calibration assembly (SRCA). MODIS reflective solar bands (RSB) calibration is reflectance based with reference to its SD bi-directional reflectance factor (BRF). The SD and SDSM are designed to operate in concert such that the changes in SD BRF can be accurately monitored by the SDSM. The thermal emissive bands (TEB) calibration is provided by the on-board BB, with its temperatures accurately measured by a set of 12 thermistors. The on-board SRCA is a unique device with multiple functions. It can be operated in different modes, allowing radiometric, spectral, and spatial characterization to be made (Xiong et al., 2003, 2009a; Xiong and Barnes, 2006).

Currently, there are two MODIS instruments operated in space, one onboard the Terra spacecraft and the other on the Aqua spacecraft. Although both Terra and Aqua MODIS instruments were built with the same design requirements and calibration approaches and went through extensive pre-launch calibration and characterization activities (Barnes et al., 1998), their on-orbit calibration consistency still needs to be carefully examined and validated as many science products are generated from observations made by both instruments. Because of this, MODIS calibration and validation scientists and the MODIS Characterization Support Team (MCST) have made significant efforts to accurately calibrate and characterize both Terra and Aqua MODIS and to inter-compare and validate their calibration consistency (Hook et al., 2007; Minnett et al., 2004; Thome et al., 2003; Wan et al., 2004; Barnes et al., 2006; Xiong et al., 2006, 2009b). Much progress has been made in recent years, but significant challenges still exist due to increasing demands for high-quality and long-term CDR.

2.2 AVHRR

The NOAA National Environmental Satellite, Data, and Information Service (NESDIS) operates two satellite systems: the Geostationary Operational Environmental Satellite (GOES) system, which observes the same area of the Earth continuously and the Polar-orbiting Operational Environmental Satellite (POES) system, which provides global observations in north-south strips at approximately the same local time (sun-synchronous). The "operational" nature of these satellites ensures long-term continuity and a guarantee of replacement in case of failure (launched approximately once every two years). The POES consists of a series of NOAA satellites named NOAA-6 to NOAA-19, from 1979 to present. They are launched into the "morning" or "afternoon" orbits, depending on their local equator crossing time, to provide the desired temporal coverage. The POES program is further expanded into the Meteorological Operational (Metop) Satellites commenced in 2006 in collaboration with the European Organization for the Exploitation of Meteorological Satellites (EUMETSAT), which becomes responsible for the morning orbits.

The AVHRRs, the prime instruments on NOAA satellites since NOAA-6, have been continuously observing the Earth for nearly 30 years. It is a traditional cross-track line scanning radiometer that measures scene radiance in the infrared (IR) and VIS/NIR spectrum. The original AVHRR had four channels. It was expanded to five and six channels in the later models. Among the six spectral channels, there are one visible (VIS) channel (1 at 0.64 μm), one near-infrared (NIR) channel (2 at 0.86 μm), one short-wave infrared (SWIR) channel (3a at 1.6 μm), one mid-wave infrared (MWIR) channel (3 or 3b at 3.7 μm), and two long-wave infrared (LWIR) channels (4 and 5 at 10.5 μm and 11.5 μm). However, only up to five channels are available at any given time with the channel switching of 3a and 3b in the late models. The instantaneous field of view (IFOV) of AVHRR is 1.3mrad square, providing a nadir footprint of 1.1 km on the Earth from a nominal altitude of 833 km. The infrared channel data from the AVHRR instruments are used for sea and land surface temperature retrievals, and cloud and fire detection, while the visible/near-infrared channels are used for cloud and snow, vegetation, aerosols, and other applications. AVHRR was initially designed for weather applications with no stringent requirement for calibration accuracy. The infrared channels are calibrated with a warm blackbody and cold space views. The VIS/NIR channels, on the other hand, have no onboard calibration and therefore vicarious calibration at desert sites is used. As nearly 30 years of satellite observations have been collected, more and more users are interested in using AVHRR data for climate

Table 1 MODIS spectral band specifications and primary applications

RSB band	CW	BW	Ltyp	SNR	primary use
1	0.645	0.050	21.8	128	land/cloud/aerosols boundaries
2	0.858	0.035	24.7	201	
3	0.469	0.020	35.3	243	land/cloud/aerosols properties
4	0.555	0.020	29.0	228	
5	1.240	0.020	5.4	74	
6	1.640	0.024	7.3	275	
7	2.130	0.050	1.0	110	
8	0.412	0.015	44.9	880	ocean color/phytoplankton/biogeochemistry
9	0.443	0.010	41.9	838	
10	0.488	0.010	32.1	802	
11	0.531	0.010	27.9	754	
12	0.551	0.010	21.0	750	
13	0.667	0.010	9.5	910	
14	0.678	0.010	8.7	1087	
15	0.748	0.010	10.2	586	
16	0.869	0.015	6.2	516	
17	0.905	0.030	10.0	167	atmospheric water vapor
18	0.936	0.010	3.6	57	
19	0.940	0.050	15.0	250	
26	1.375	0.030	6.0	150	cirrus clouds water vapor
TEB band	CW	BW	Ttyp	NEdT	primary use
20	3.75	0.18	300	0.05	surface/cloud temperature
21	3.96	0.06	335	0.20	
22	3.96	0.06	300	0.07	
23	4.05	0.06	300	0.07	
24	4.47	0.07	250	0.25	atmospheric temperature
25	4.52	0.07	275	0.25	
27	6.72	0.36	240	0.25	water vapor
28	7.33	0.30	250	0.25	
29	8.55	0.30	300	0.05	cloud properties
30	9.73	0.30	250	0.25	ozone
31	11.03	0.50	300	0.05	surface/cloud temperature
32	12.02	0.50	300	0.05	
33	13.34	0.30	260	0.25	cloud top altitude
34	13.64	0.30	250	0.25	
35	13.94	0.30	240	0.25	
36	14.24	0.30	220	0.35	

Note: CW and BW are center wavelength and bandwidth in μm; Ltyp is typical radiance in $W/(m^2 \cdot sr^{-1} \cdot \mu m^{-1})$; Ttyp is typical temperature in Kelvin (K); SNR is signal-to-noise ratio; NEdT is noise equivalent difference temperature in K

studies, where a small calibration bias can lead to very different conclusions about the global climate change. Many efforts have been devoted to improving the calibration of AVHRR for long-term time series analysis in recent years and several publications are available to address the AVHRR onboard calibration issues (Brown et al., 1985; Cao et al., 2001, 2004a; Steyn-Ross et al., 1992; Rao and Chen, 1999; Trishchenko, 2002; Trishchenko et al., 2002; Walton et al., 1998).

2.3 ETM+

To date, the Landsat program has surpassed three decades of imaging the Earth's surface. Landsat 1 (L1), Landsat 2 (L2), and Landsat 3 (L3), with the Multispectral Scanner (MSS) sensor and the Return Beam Vidicon (RBV) camera as payloads on a "NIMBUS-like" platform were launched in July 1972, January 1975, and March 1978, respectively. The MSS sensor has four spectral bands in the VIS and

NIR regions with spatial resolution of approximately 79 m. Landsat 4 (L4) and Landsat 5 (L5), which carry the Thematic Mapper (TM) sensor as well as the MSS on the Multimission Modular Spacecraft, were launched in July 1982 and March 1984, respectively. Landsat 6 (L6) and Landsat 7 (L7), which include the Enhanced Thematic Mapper (ETM) and the Enhanced Thematic Mapper Plus (ETM+), were launched in October 1993 and April 1999, respectively. Landsat 6 failed on launch. L5 TM and L7 ETM+ sensors are still operational. The L5 TM incorporated advancements in spectral, radiometric, and geometric capabilities over its predecessors with six reflective bands (1–5 and 7) centered at 0.49, 0.56, 0.66, 0.83, 1.67, and 2.24 μm and one thermal IR (TIR) band (6) 11.4 μm. The TM sensor has a spatial resolution of 30 m for the reflective bands and 120 m for the thermal IR band. The detectors for bands 1–4 are located on the Primary Focal Plane (PFP) with no temperature control. The detectors for bands 5–7 are located at the Cold Focal Plane (CFP) with its temperature controlled between 95 and 105 K via a passive radiative cooler. The Internal Calibrator (IC) is incorporated as an onboard radiometric calibration system for the L5 TM. Onboard calibration of the MSS and TM uses lamps for the reflective bands and a blackbody for the thermal band.

The ETM+ sensor was developed based on the TM sensors onboard the L4 and L5 satellites. Changes in the ETM+ sensor include a new panchromatic band (8), an increase in the spatial resolution of the TIR spectral band to 60 m, and two additional calibration devices: a Full Aperture Solar Calibrator (FASC), which is a white painted diffuser panel, and a Partial Aperture Solar Calibrator (PASC), which is a set of optics that allows the ETM+ to image the Sun through small apertures (holes). One of the requirements of the L7 mission is to achieve 5% radiometric calibration accuracy for the ETM+ at-sensor radiance (Markham et al., 2004). The Landsat is an invaluable resource for monitoring global change and is a primary source of medium spatial resolution Earth observations used in decision-making (Vogelmann et al., 2001; Woodcock et al., 2001; Cohen and Goward, 2004; Goward et al., 2006; Masek et al., 2008; Wulder et al., 2008).

Since the relative spectral response (RSR), also known as the spectral response function (SRF), is a key sensor calibration and retrieval parameter and plays an important role by helping to understand and assess the calibration differences among sensors, an example of MODIS/Terra, AVHRR/NOAA-17, and ETM+/Landsat-7 RSR are presented in Fig. 1. In addition to having more spectral bands, MODIS RSR bandwidths are generally narrower than for

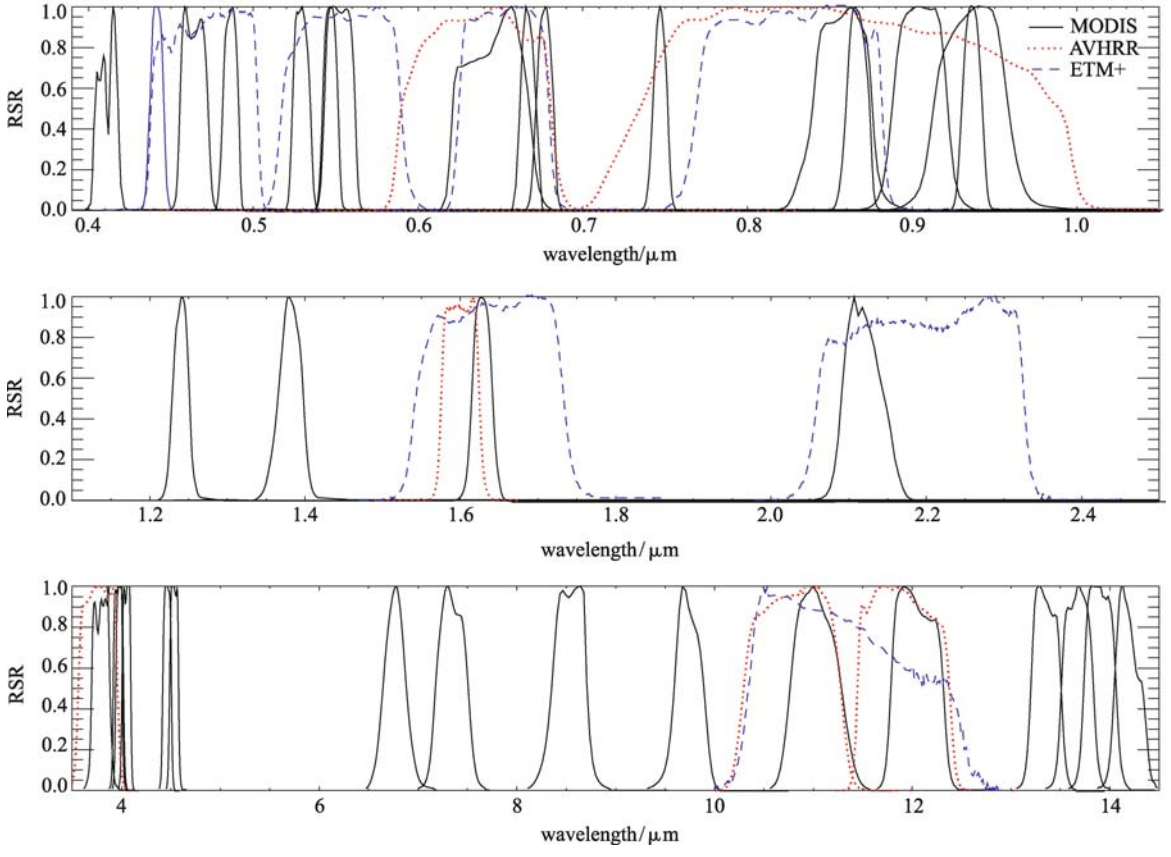

Fig. 1 Relative spectral responses (RSR) of Terra MODIS, NOAA-17 AVHRR, and Landsat 7 ETM+

its heritage sensors. For reference purposes, a summary of key satellite and sensor parameters are provided in Table 2, including Terra and Aqua MODIS, NOAA-16, -17, and-18 AVHRR, and Landsat-5 TM and Landsat-7 ETM+.

3 Inter-comparison methodologies

Given a sensor's typical design life of about five years, the detection of decadal climate change relies on observations from a series of satellites. Despite the best effort in pre-launch and post-launch calibration, radiometers on different satellites do not necessarily produce consistent measurements, even if they share the same instrument design. These inter-satellite biases, which could be very difficult to characterize due to the lack of SI traceable onboard calibration reference or standard, and the variable nature of biases both short-term and long-term, in response to the spacecraft and instrument operating conditions, have become major concerns in constructing time series for climate change detection. As a result, a number of approaches have been developed and implemented in order to better quantify these inter-satellite biases. Described in the following are the calibration inter-comparison methodologies of using "invariant" ground targets, simultaneous nadir overpass (SNO), and inter-mediate transfer sensor, and the Moon.

3.1 Ground targets

Ground targets developed for vicarious calibration or validation can be used for calibration inter-comparison between sensors. These sites are selected based on a number of factors, such as their locations, surface spatial uniformity and temporal stability, the atmospheric conditions, and, if possible, ground calibration data availability, quality, and reference traceability. Figures 2 and 3 are the satellite images over the Concordia Dome (Dome C) and Libya-4 desert areas. The Dome C site (75.1°S, 123.4°E) in Antarctica, located at an elevation of 3215 m above sea level, has been recognized as having great potential for sensor calibration inter-comparison due to several favorable factors (Six et. al., 2004; Wenny and Xiong, 2008). It is relatively uniform in both albedo and temperature with atmospheric conditions being exceptionally cold, dry, and rarefied, as well as consistently low in fractional cloud coverage. In addition, there are routine ground-based measurements of atmospheric parameters, such as air temperature, barometric pressure, and wind speed/direction information. Libya-4 is a high reflectance site located in the Libyan Desert in Africa (28.6°N, 23.4°W) at an elevation of 118 m above sea level. The Libyan Desert site is made up of sand dunes with no vegetation. Aerosol loading is typically low. Libya-4 also exhibits significant spatial, spectral, and temporal uniformity and has minimal

Table 2 Key satellite and sensor parameters for Terra and Aqua MODIS, NOAA-16, -17, and -18 AVHRR, Landsat 5 TM, and Landsat 7 ETM+

satellite/sensor	launch date	altitude/km	crossing time	No. of bands
Terra / MODIS	Dec. 18 1999	705	10:30 AM	36
Aqua / MODIS	May 04 2002	705	1:30 PM	36
NOAA-16 / AVHRR	Sept. 21 2000	850	1:40 PM	6
NOAA-17 / AVHRR	June 24 2002	850	10:20 AM	6
NOAA-18 / AVHRR	May 20 2005	870	1:40 PM	6
Landsat-5 / TM	March 1 1984	705	9:45 AM	7
Landsat-7 / ETM+	April 15 1999	705	10:00 AM	8

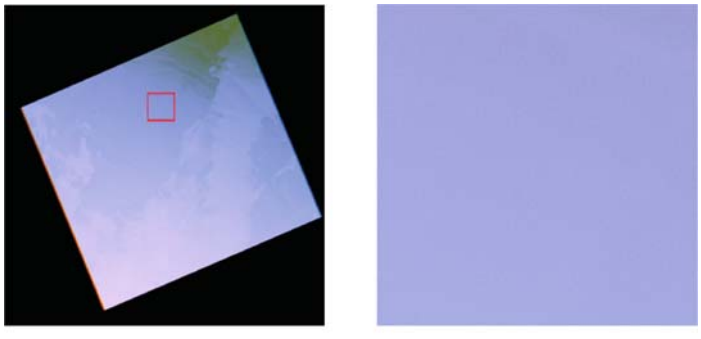

Fig. 2 Full resolution (a) and zoomed (b) color images from ETM+ bands 3, 2, and 1 acquired on 3 January 2000 over the Dome-C site. The rectangular box indicates the zoom location of the center latitude and longitude of the Dome-C site

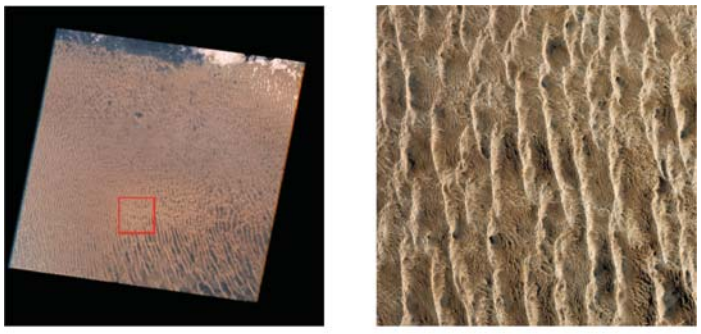

(a) (b)

Fig. 3 Full resolution (a) and zoomed (b) color images from ETM+ band 3, 2, and 1 acquired on 31 May 2003 over the Libya-4 site. The rectangular box indicates the zoom location of the center latitude and longitude of the Libya-4 site

cloud cover. The above characteristics have made the Libya-4 site a favorite candidate for sensor stability monitoring (Rao and Chen, 1999; Cabot et al., 1999, 2000; Chander et al., 2009).

In sensor vicarious calibration or validation, the measured TOA reflectance factor or at-sensor spectral radiance is compared with the projected quantity either predicted from a model or derived from ground measurements. Applying the same procedure to sensors A and B yields the ratios (r_A and r_B) of the sensor measured to the projected values, or the differences (d_A and d_B) between them,

$$r_A = I_{A\_Mea}/I_{A\_Proj} \quad \text{and} \quad r_B = I_{B\_Mea}/I_{B\_Proj}, \quad (1)$$

or

$$d_A = I_{A\_Mea} - I_{A\_Proj} \quad \text{and} \quad d_B = I_{B\_Mea} - I_{B\_Proj}, \quad (2)$$

where I_{A_Mea} and I_{B_Mea} are the TOA reflectance factors or the at-sensor spectral radiance from sensor A and B measurements, and I_{A_Proj} and I_{B_Proj} are the projected values. For a closely matched spectral band pair on sensors A and B, the ratio (r_{AB}) of r_A and r_B or the difference (d_{AB}) between d_A and d_B can be used effectively to assess their calibration consistency,

$$r_{AB} = r_A/r_B \quad \text{and} \quad d_{AB} = d_A - d_B. \quad (3)$$

3.2 Simultaneous nadir overpasses (SNO)

Since each satellite passes most locations on the earth at different times, inter-comparison of observations from any pair of satellites has uncertainties due to differences in their solar zenith and view angles. The cloud and air mass movement and diurnal cycles in the natural phenomena introduce additional uncertainties. In general, large uncertainties exist when comparing observations from two satellites in different orbits. In order to eliminate or reduce these uncertainties, the simultaneous nadir overpass (SNO) approach was developed and applied to inter-satellite comparisons (Cao and Heidinger, 2002; Herdinger et al., 2002). Because of orbital time period differences, any pair of earth orbiting satellites with different altitudes passes the same place or views the same ground target at the same time regularly, which creates opportunities for inter-satellite comparisons with greatly reduced uncertainties. Figure 4 is an example of an SNO image pair of MODIS on Aqua and AVHRR on Metop-A.

Given a pair of earth orbiting satellites, their orbital perturbation can be calculated accurately with such models

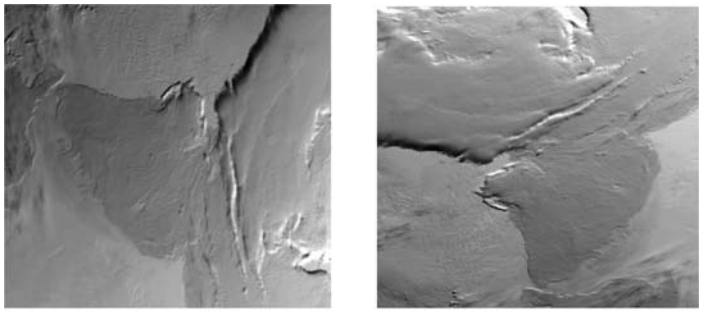

(a) (b)

Fig. 4 An SNO image pair from Metop-A AVHRR channel 1 (a) and Aqua MODIS band 1 (b) acquired on 13 December, 2006 (2006347.2345)

as SGP4 (Simplified General Perturbations Satellite Orbit Model 4), and their orbital intersections can be predicted accurately for approximately two weeks in advance through numerical analysis (Cao et al., 2004b). The predicted time and location are then used to find the exact orbit in the Level 1B (L1B) data from satellite observations. The precise location and time of the SNO can then be found from the two intersecting orbits, given a typical time difference criteria of 30 seconds passing the same location at nadir. After the SNO method was initially developed, it has been applied to the inter-comparison/inter-calibration for a variety of radiometers, ranging from visible, near infrared, and infrared to microwave instruments with great success. For a closely matched spectral band pair on sensors A and B, the ratio (r_{AB}) of their measured quantities, I_{A_Mea} and I_{B_Mea}, or the difference (d_{AB}) between I_{A_Mea} and I_{B_Mea}, is used to examine their calibration difference,

$$r_{AB} = I_{A\_Mea}/I_{B\_Mea} \quad \text{and} \quad d_{AB} = I_{A\_Mea} - I_{B\_Mea}. \quad (4)$$

For additional improvements, the results from a direct SNO approach (Eq. (4)) should be corrected for the relative spectral response (RSR) difference between the two spectrally matched bands of sensors A and B. The correction factor also varies with the Earth view scene type.

3.3 Intermediate transfer sensor

For satellites orbiting at the same altitude, there is no SNO opportunity. This is the case for the Terra and Aqua satellites, and the Landsat 5 and Landsat 7 satellites. Because of this, the SNO approach cannot be directly applied to inter-compare Terra and Aqua MODIS calibration. On the other hand, it has been recognized that both Terra and Aqua MODIS can be directly inter-compared to a common "third" sensor via SNO. Thus, the difference between the third sensor's comparisons with both Terra and Aqua MODIS reflects the calibration difference between the two MODIS instruments. This is a two-step approach, which takes the advantages of SNO. It has been regularly used by the MODIS Characterization Support Team (MCST) to monitor Terra and Aqua MODIS calibration differences (Wu et al., 2003, 2008; Xiong et al., 2008). In this approach the common "third" sensor, serving as a transfer radiometer, must be stable during the time between its comparisons with the other sensors. Equations 1–3 can be modified for this approach by replacing the projected values I_{A_Proj} and I_{B_Proj} with the observed quantities of the third sensor, C, at the times of its SNO with sensors A and B.

3.4 Lunar observations

Since its surface reflectance property is known to be extremely stable, the Moon, or the sunlight reflected from the lunar surface, has been used to track sensor radiometric calibration stability in the VIS/NIR spectral regions (Barnes et al., 2006; Eplee et al., 2006; Sun et al., 2007; Xiong et al., 2008). Since launch, the SeaWiFS instrument has collected more than 130 lunar views at a phase angle of approximately 7 degrees and used these lunar observations to calibrate the long-term changes in its detector responses. Lunar observations also serve as a key component of MODIS on-orbit calibration strategies for its RSB. They are scheduled on a near-monthly basis at nearly the same phase angles: [−56°, −55°] for Terra MODIS and [55°, 56°] for Aqua MODIS when the sensors are on the night side of the Earth. A series of Terra MODIS lunar images are displayed in Fig. 5.

Although it is highly stable in terms of its surface reflectance property, the lunar surface uniformity has not been adequately characterized for radiometric calibration purposes. Consequently, the integrated irradiance over the entire lunar surface is often used to monitor sensor calibration stability. Furthermore, the integrated lunar irradiance derived from sensor observations must correct the effect due to the Sun-Moon and Moon-satellite distances and lunar viewing geometry, including its phase and libration angles. This correction can be made by normalizing the sensor-observed lunar irradiance to the model predicated value under the same observation condition. The Robotic Lunar Observatory (ROLO) model developed at the USGS has been used for MODIS and SeaWiFS instruments and other earth observing

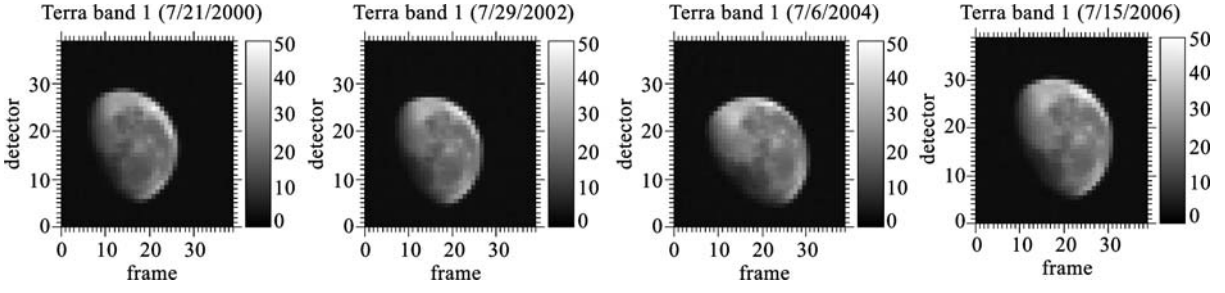

Fig. 5 A set of lunar images from Terra MODIS band 1 (all detectors in one scan) acquired in July of 2000, 2002, 2004, and 2006

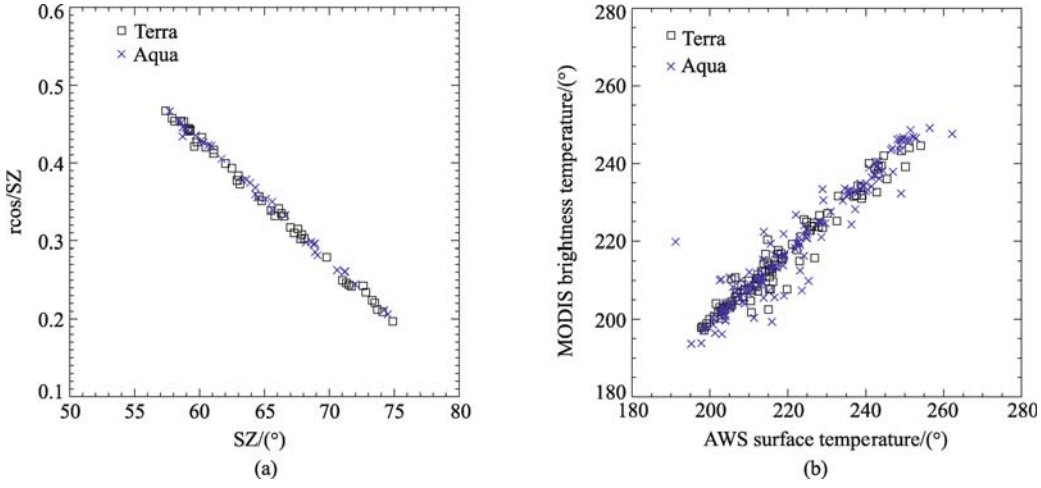

Fig. 6 (a) MODIS band 1 TOA reflectance factors (from October 2002 to February 2003) versus solar zenith angles and (b) band 31 brightness temperatures (from July 2002 to June 2003) versus AWS surface temperatures over the Dome C site

sensors (Kieffer and Stone, 2005). The calibration consistency of a closely matched spectral band pair from sensors A and B can be evaluated by

$$r_{AB} = \{I_{A\_Mea}/I_{A\_Model}\}/\{I_{B\_Mea}/I_{B\_Model}\}, \quad (5)$$

where I_{A_Mea} and I_{B_Mea} stand for the sensor A and B measured lunar irradiances, and I_{A_Model} and I_{B_Model} stand for the corresponding model-predicted values.

4 Applications and results

4.1 Ground targets

Ground targets are often used to vicariously calibrate the Earth-observing sensors, especially the sensors without onboard calibrators in the VIS and NIR spectral regions. These sites are selected based on their "favorable" or "well-characterized" surface properties. For example, the Dome C site has been extensively used in recent years for the long-term trending of Terra and Aqua MODIS calibration consistency (Xiong et al., 2009b). Figure 6(a) shows MODIS band 1 (0.645 μm) top of atmosphere (TOA) reflectance factors as a function of solar zenith angles using near nadir observations made over the Dome C during a period in 2002–2003. A similar plot of band 31 (11 μm) brightness temperatures versus the surface temperatures from an Automated Weather Station (AWS) is illustrated in Fig. 6(b). For the VIS/NIR spectral bands, a simple approach can be used to estimate Terra and Aqua calibration difference using ratios of their observed (nadir) reflectance factors at common solar zenith angles. An alternative approach is to apply a BRDF model, such as the one developed based on in-situ near-surface measurements of the snow surface in Antarctica (Warren and Brandt., 1998), for the normalization. In this study, the model coefficients are derived from a best fit to both sensors' observations made during the first year of their overlapped mission (October 2002-February 2003) and applied to their entirely overlapped mission. The yearly averaged results, ratios of sensor-observed to the model-predicated BRF and their standard deviations, are presented in Fig. 7 for MODIS bands 1 (0.645 μm) and 2 (0.858 μm). There are

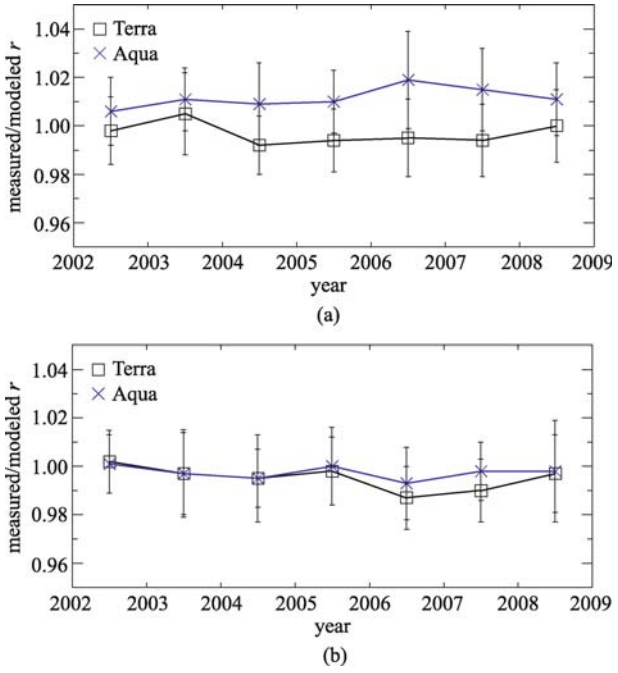

Fig. 7 Calibration inter-comparison of Terra and Aqua MODIS band 1 (a) and band 2 (b) using observations over Dome C with references to a ground surface BRDF model

approximately 80 overpasses each year used in this study. The results indicate that the Terra and Aqua MODIS band 1 calibration difference is less than 2.0% over their entire mission, with Terra measured BRF being higher than Aqua, and the calibration change in each sensor has been less than 1%. For MODIS band 2, the agreement between the two sensors is better than 1% and the change in their calibration difference is less than 0.5%. Overall, the long-term trending of their calibration has been very stable. For the TIR spectral bands, the sensor observations can be referenced to the coincident AWS measurements. There is an apparent temperature difference between the TOA brightness temperature observed by the sensor and surface temperature measured by the AWS. Since this difference is the same for both Terra and Aqua MODIS window channels at 11 and 12 μm, no additional correction is necessary in deriving their calibration differences as both sensors' RSR are nearly identical. Their yearly averaged temperature differences and standard deviations are illustrated in Fig. 8. Large standard deviations are primarily due to the fact that the difference between the TOA brightness temperature and surface temperature is seasonally dependent. For a temperature range of 190–250 K, the calibration differences between Terra and Aqua MODIS at 11 and 12 μm are typically less than 20 mK. This approach can be easily applied to other sensors.

Using observations made over the Libyan Desert site, Figure 9 displays the yearly averaged calibration trends of Terra MODIS bands 1 and 2 and the corresponding Landsat ETM+ bands 3 and 4. Approximately 100 overpasses (near simultaneous) over this site are included in this analysis. The normalization is also made via a BRDF model (Schaaf et al., 2002), different from the one used for the Dome C site, with its coefficients derived from initial Terra MODIS observations. In general, the BRDF model is selected based on the surface types of the ground targets. The results in Fig. 9 show that the observed radiance (or reflectance factor) of MODIS band 1 is about 5% higher than ETM+ band 3 while MODIS band 2 is nearly 3.5% lower than ETM+ band 4. Some of the apparent calibration differences are due to their RSR difference and can be estimated using either the standard RTM or the observed spectra from a hyper-spectral sensor. In this case, applying corrections for the RSR difference leads to smaller calibration differences.

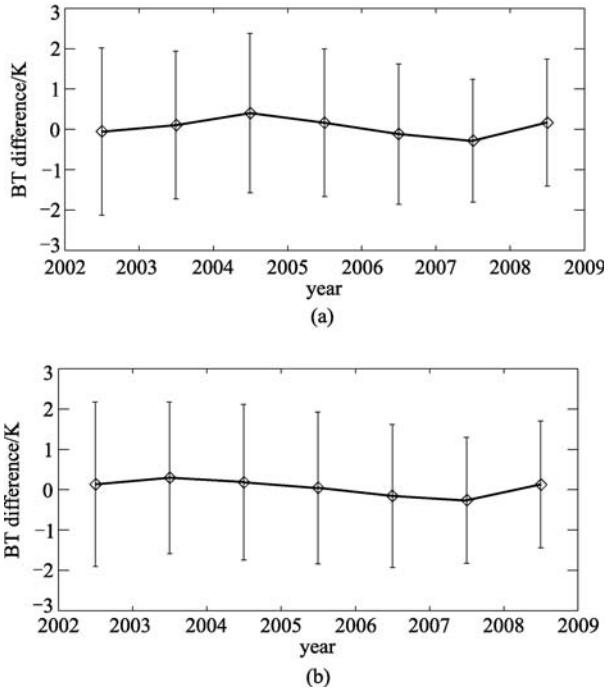

Fig. 8 Calibration difference between Terra and Aqua MODIS band 31 (a) and band 32 (b) determined from observations over Dome C

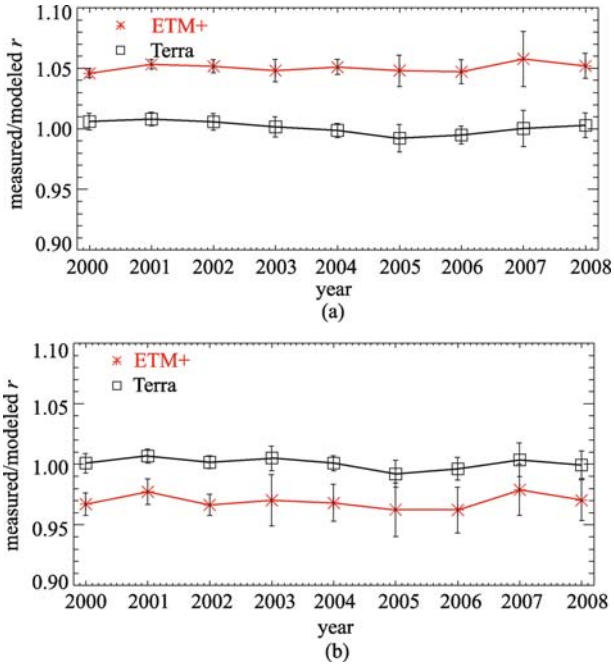

Fig. 9 Calibration inter-comparison of Terra MODIS band 1 (a) and band 2 (b) and corresponding Landsat 7 ETM+ bands using observations over Libya-4 Desert site with references to a ground surface BRDF model

4.2 SNO

Over the years, much progress has been made in applying the SNO method to the same and different types of radiometers. In particular, applications of the SNO method to microwave instruments have produced very promising results for climate change detection. Several factors contribute to this success. First, the inter-satellite biases for microwave instruments appear to change little over the short-term and slowly over the long-term. Second, the microwave channel center frequencies between instruments are made to match precisely with little or no "spectral"

differences. And third, each microwave instrument has its own onboard blackbody calibration, which keeps tracking the instrument degradation independently. The SNO method works especially well for microwave instruments sensing the mid-troposphere to upper stratosphere. For applications to the VIS/NIR radiometers, such as those on the AVHRR and MODIS, recent studies show that the SNO method can reduce the inter-comparison uncertainties down to±1% for channels with very similar spectral response functions (Cao et al., 2008) and is very effective in quantifying the inter-satellite biases for these channels. Since the biases are short-term invariant for the VIS/NIR instruments, they can be used for inter-calibrating the satellites for the global data. The dry atmosphere and highly reflective surface for a broad range of solar zenith angles at the SNO sites in Polar Regions are advantageous for calibrating these channels.

Figure 10 shows that the agreement in the calibration between NOAA-16 and -17 AVHRR channel 2 (0.86 μm) has become much better after the calibration coefficients for NOAA-17 were updated, although a small difference still exists after the update. Since the SNO method only provides a relative calibration between two satellites and none of the NOAA-satellites has on-board calibration for the VIS/NIR channels, the SNO calibration alone is not sufficient to produce a long-term time series for these channels. This method is more useful if one satellite can be relied on as a stable standard, such as in the inter-calibration of MODIS and NOAA radiometers (Heidinger et al., 2002), but the difference in the spectral response functions between them introduces uncertainties.

For each SNO event, Eq. (4) is applied to the spatially matched pixels from both sensors over uniform areas. Typically, a ratio is used for the reflectance factors in the VIS/NIR region and a difference is used for the brightness temperatures in the TIR region. Figures 11 and 12 are examples of using MODIS as a reference and SNO to inter-calibrate AVHRR on NOAA-16, 17, and 18. There are clear calibration differences between MODIS and AVHRR for the VIS channel at 0.645 μm. Some biases are expected due to their RSR differences and some are likely due to their calibration differences. MODIS is calibrated using its onboard solar diffuser (with a stability monitor) and AVHRR has been traditionally calibrated using either its pre-launch calibration coefficients or the ones updated from vicarious calibration over a desert site. The differences in the TIR channel at 11 μm are much smaller because both sensors are calibrated using their onboard

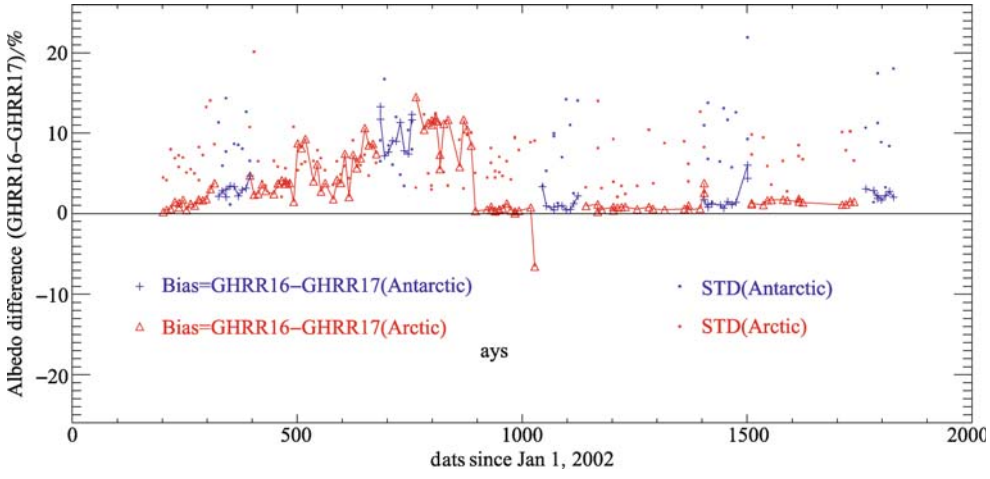

Fig. 10 SNO time series showing improved agreement between NOAA-16 and -17 AVHRR channel 2 (0.86 μm) calibrations after the NOAA-17 AVHRR coefficient update in June 2004

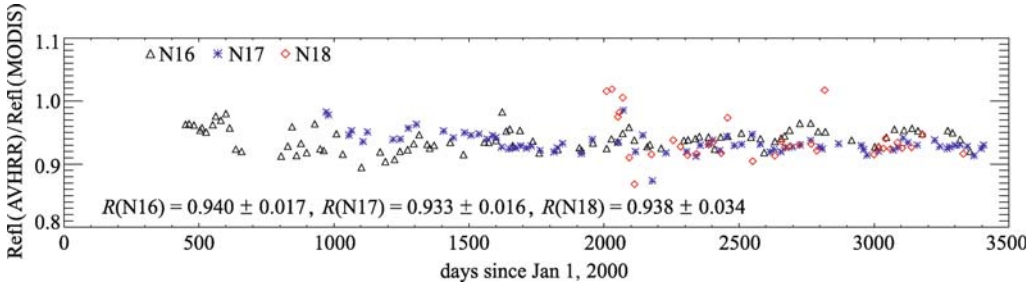

Fig. 11 SNO time series of inter-comparison of Terra MODIS band 1 and NOAA-16, -17, -18 AHVRR channel 1

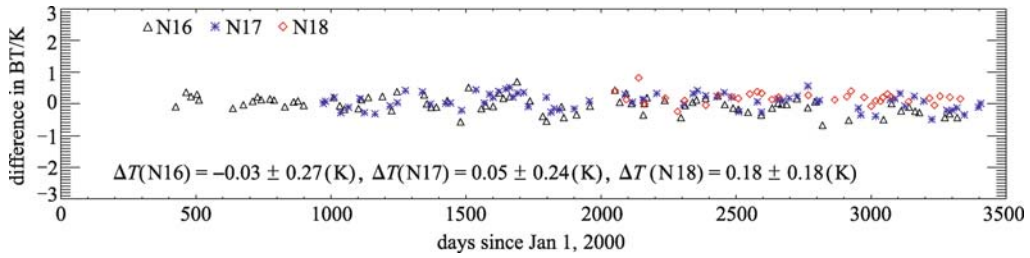

Fig. 12 SNO time series of inter-comparison of Terra MODIS band 31 and NOAA-16, -17, -18 AHVRR channel 4

blackbody. The SNO approach is extremely effective in quantifying the differences of both short- or long-term among AVHRR instruments since the same stable MODIS instrument is used as the reference. For infrared channels, studies have shown that the SNO method can quantify inter-satellite biases with uncertainties smaller than the instrument noise (Cao and Heidinger, 2002).

4.3 Intermediate transfer sensor

As previously described, a third sensor, serving as the intermediate transfer radiometer, can be used to inter-compare a pair of sensors, which may not have direct SNO opportunities due to their orbital constraints. Typically, the third sensor is operated at a different altitude and thus could have SNO opportunities with the other two sensors that need to be inter-compared. Using an AVHRR instrument as the transfer radiometer, this approach has been applied to inter-compare Terra and Aqua MODIS (Xiong et al., 2006). Since AVHRR channels 1, 2, 4, and 5 are closely matched with MODIS spectral bands 1, 2, 31, and 32 at 0.65, 0.86, 11, and 12 μm, respectively, and both Terra and Aqua MODIS RSR are nearly identical, no additional spectral correction is needed if the ground targets are of the same type.

Figure 13 shows the SNO inter-comparison results of MODIS band 1 with AVHRR (on NOAA-16) channel 1 at 0.65 μm. Using this approach, the averaged calibration difference between Terra and Aqua MODIS band 1, from 2002 to present, is about 1.5%. This is within the 2% calibration accuracy requirement for MODIS reflective solar bands. The results in Fig. 13 are consistent with those derived from the Dome C approach shown in Fig. 9. Using the same approach, inter-comparison results at 11 μm are illustrated in Fig. 14 in terms of TOA brightness temperature differences. On average, the Aqua MODIS calibration is about 20 mK lower than Terra MODIS at 11 μm. The calibration difference in the TIR region often depends on the scene temperatures. It is not surprising that similar results are obtained using AVHRR sensors on different platforms (Wu et al., 2008).

Other sensors can also be used as the intermediate

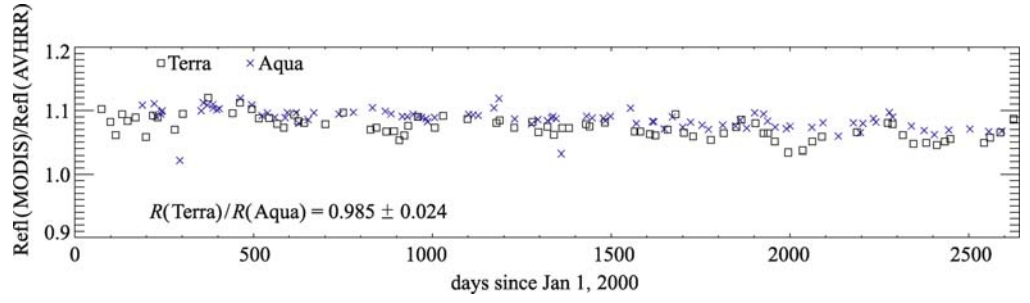

Fig. 13 Calibration inter-comparison of Terra and Aqua MODIS band 1 using NOAA-16 AVHRR channel 1 as a common reference

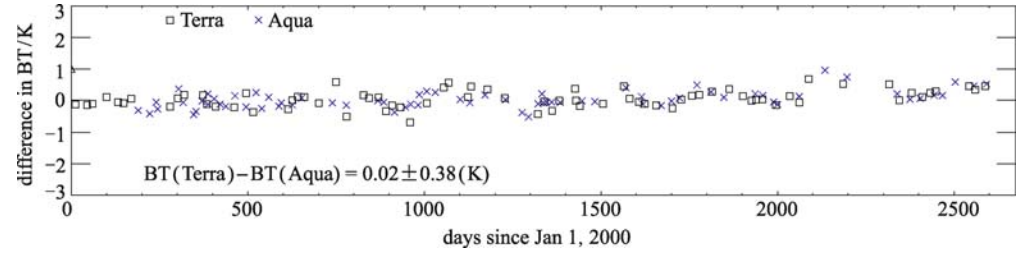

Fig. 14 Calibration inter-comparison of Terra and Aqua MODIS band 31 using NOAA-16 AVHRR channel 4 as a common reference

transfer radiometer for Terra and Aqua MODIS calibration inter-comparison. If the transfer radiometer's RSR is quite different from MODIS and the SNO ground target types are different, corrections must be made to the sensor observed TOA reflectance factors and radiances, regardless of the similarity of both Terra and Aqua MODIS.

4.4 Lunar observations

Lunar observations have been successfully exploited by a number of sensors, such as MODIS and SeaWiFS, to track their on-orbit calibration stability or changes in responses in the VIS/NIR spectral regions (Barnes et al., 2006). For calibration inter-comparison purposes, the Moon is considered to be an extremely stable reference, apart from the effects due to lunar view geometries. Because of this, the lunar observations have been considered a required capability in the design of a number of new sensors, including the NPOESS Visible/Infrared Imager Radiometer Suite (VIIRS), LDCM Operational Land Imager (OLI), and GOES-R Advanced Baseline Imager (ABI). Although a lunar model, such as the USGS ROLO model, can provide the predicted lunar irradiances (integrated over the entire lunar surface), lunar observations by each sensor should be made, if possible, at the same phase angle in order to reduce the uncertainties caused by the lunar viewing geometry differences. Consequently, the scheduled lunar observations often require spacecraft maneuvers. For example, MODIS lunar observations are made through its space view port with spacecraft roll maneuvers and SeaWiFS lunar observations via pitch maneuvers. Because of operational constraints, the roll angles for MODIS lunar observations are constrained between 0° and −20°. In addition, MODIS lunar observations are made during the spacecraft night-time.

Figure 15(a) illustrates the observed lunar irradiances by both Terra and Aqua MODIS band 1 over a three-year period. As a comparison, the model predicted lunar irradiances under the same viewing conditions are also presented. Similar results for bands 2 and 3 (0.469 μm) are shown in Figs. 15(b) and (c). There is a clear spectrally dependent difference between the observed and modeled results. The difference, however, should not prevent lunar observations from being effectively used for calibration inter-comparison. Applying Eq. (5), the Terra and Aqua MODIS calibration differences for bands 1–3 are presented in Fig. 15(d). Initial inter-comparison results are within ±1%. After removing the apparent seasonal features, common to all spectral bands, the inter-comparison results can be significantly improved to a fractional percent. It should be pointed out that MODIS is a cross-track scanning radiometer and its lunar observations are made through its SV port at an Angle of Incidence (AOI) of 10.2°. Since its on-orbit solar calibration is made at an AOI of 50.2°, MODIS lunar observations are used to track the changes in sensor response versus scan angle (Sun et al., 2007).

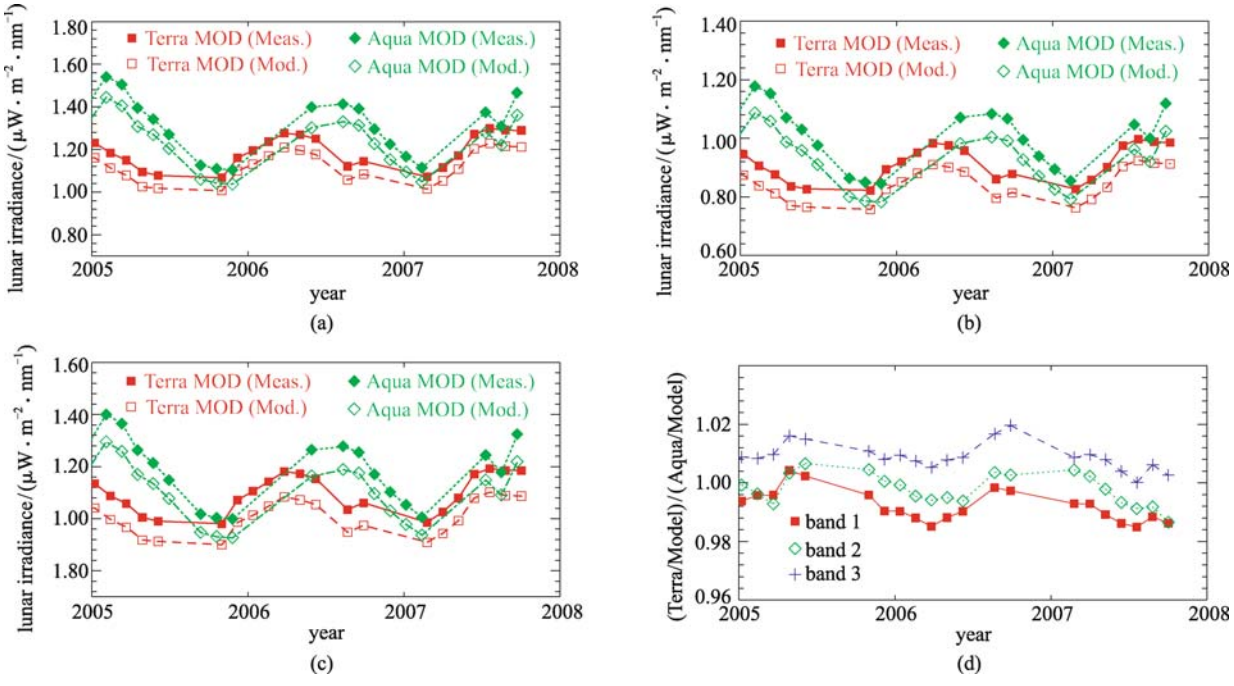

Fig. 15 Measured and model predicated lunar irradiances of Terra and Aqua MODIS band 1 (a), band 2 (b), and band 3(c), and Terra and Aqua MODIS calibration differences (d) for bands 1, 2, and 3 (results normalized to the model predicated lunar irradiances)

5 Discussion

Although each of the methods described above can be effectively implemented for sensor calibration inter-comparisons depending on their specific applications, they are not without limitations. As discussed in all cases, the spectral difference between sensors must be carefully considered and properly corrected, unless there is a perfect match. For the ground target approach, the changes, even at a very slow rate, of the site surface characteristics and atmospheric conditions will impact the inter-comparison quality. In this approach, a time series constructed from frequent satellite observations are often needed to establish the long-term trend and identify the calibration difference among multiple sensors. This approach is not adequate for studying the sensor short-term calibration difference unless there are simultaneous ground-based measurements that can be used to characterize the different conditions.

The SNO approach uses observations made at the same time over the same target by each sensor pair. However, these observations often occur at many different locations in the polar region and the spectral characteristics of the SNO sites are currently not well quantified, which could introduce additional uncertainties for the calibration inter-comparison. While the SNO method works well for the sounding channels in the microwave and infrared, it does not work as well for the surface channels where inhomogeneity becomes a major factor for these instruments. For the infrared window channels of some sensors, the temperature at the SNO is often limited to a narrow range that does not cover the full range of the global surface temperature. In addition, the inter-satellite biases at the SNO points may not be representative of the biases over an orbit due to orbital variations of calibration accuracy in response to fluctuations in instrument temperature and stray light in certain parts of the orbit. Finally, the SNO method is very sensitive to geolocation and sampling errors. For example, the AVHRR 5 km GAC data does not match with the MODIS 1 km data due to the sampling scheme used in AVHRR, which introduces additional uncertainties in inter-calibrating AVHRR and MODIS.

The third sensor approach requires the reference sensor to be very stable between its SNO with the other sensors. The inter-comparison uncertainties will be relatively large if the sensors involved have different spectral responses, as two corrections for the spectral differences are needed. It works very well, however, if the two sensors to be compared are nearly the same, such as Terra and Aqua MODIS.

The lunar approach offers many advantages, in terms of stability, spectral normalization, and atmospheric effect, but may not be readily available for all sensors, past and present. Although the Moon has been effectively used for tracking sensor calibration stability, extensive research efforts are still needed before the Moon can be used as an absolute calibration source. In order to further reduce the uncertainties due to different lunar viewing geometries, the lunar observations from each sensor should be made at the same phase. This, however, often requires spacecraft maneuvers, such as the pitch maneuvers made by the SeaWiFS satellite and the roll maneuvers made by the Terra and Aqua spacecrafts. There could be up to 1% inter-comparison uncertainty if lunar observations were made at different phase angles.

In addition to corrections for the spectral response difference, atmospheric impact, spatial and sampling effects, the combined impact due to scene polarizations and sensors' polarization sensitivity need to be considered for future high quality calibration inter-comparison studies. Considerations must also be made at the sensor design phase, including high quality system level characterization of sensor RSR, polarization sensitivity, and instrument temperature sensitivity. Pre-launch calibration must firmly establish the traceability to the national or international standards with well documented and quantified uncertainty assessments for all components on the calibration chain. It is also equally important to transfer pre-launch calibration to on-orbit without breaking the chain of calibration traceability and uncertainty. Currently, there are a number of major sensors/missions in various phases of design and development. Compared to their heritage sensors, many improved requirements have been added in the new sensors. Considerations, such as calibration traceability and lunar observation capability, have been addressed, in support of future high quality sensor calibration inter-comparison studies.

6 Summary

High quality sensor calibration inter-comparison will continue to play an important role as more and more satellite observations are used for science applications and climate studies. Though much progress has been made in recent years, major challenges remain to be overcome in order to firmly establish the calibration traceability, or reference scale, among sensors and to constantly track their calibration stability throughout their entire missions. This paper provides an overview of key methodologies, which have been successfully implemented for sensor calibration inter-comparison with demonstrated potential of improving the quality of long-term climate data records (CDR), including the use of ground targets, near simultaneous nadir overpasses (SNO), intermediate transfer sensors, and the Moon. Applications of different methodologies are illustrated using examples from the most popular and widely used sensors, such as MODIS, AVHRR, and ETM+. Limitations of each methodology and further improvements are also presented in this paper. It is

expected that the methodologies and examples presented in this paper will benefit future sensor inter-comparison studies.

Acknowledgements The authors would like to thank Amit Angal and Aisheng Wu of the MODIS Characterization Support Team (MCST) for technical assistance and contributions to the analysis.

References

Barnes W L, Pagano T S, Salomonson V V (1998). Prelaunch characteristics of the Moderate Resolution Imaging Sectroradiometer (MODIS) on EOS-AM1. IEEE Trans Geosci Remote Sensing, 36: 1088–1100

Barnes W L, Salomonson V V (1993). MODIS: A global image spectroradiometer for the Earth Observing System. Critical Reviews of Optical Science and Technology, CR47: 285–307

Barnes W L, Xiong X, Eplee R, Sun J, Lyu C H (2006). Use of the Moon for calibration and characterization of MODIS, SeaWiFS, and VIRS. Earth Science Satellite Remote Sensing, 2: 98–119

Brown O B, Brown J, Evans R (1985). Calibration of advanced very high resolution radiometer infrared observations. J Geophys Res, 90 (C6): 11667–11677

Cabot F, Hagolle O, Henry P (2000). Relative and Multi-Temporal Calibration of AVHRR, Seawifs, and Vegetation Using POLDER Characterization of Desert Sites. Proceedings of IGARSS, 2000: 2188–2190

Cabot F, Hagolle O, Ruffel C, Henry P (1999). Use of remote sensing data repository for in-flight calibration of optical sensors over terrestrial targets. Proceedings of SPIE 3750: 514–523

Cao C, Heidinger A (2002). Inter-Comparison of the Longwave Infrared Channels of MODIS and AVHRR/NOAA-16 using Simultaneous Nadir Observations at Orbit Intersections. Proceedings of SPIE 4814: 306–316

Cao C, Sullivan J, Maturi E, Sapper J (2004a). The effect of orbit drift on the calibration of the 3.7 um channel of the AVHRR onboard NOAA-14 and its impact on night-time sea surface temperature retrievals. Int J Remote Sens, 25(5): 975–986

Cao C, Weinreb M, Sullivan J (2001). Solar Contamination Effects on the Infrared Channels of the AVHRR. J Geophys Res, 106(No D24): 33463–33469

Cao C, Weinreb M, Xu H (2004b). Predicting simultaneous nadir overpasses among polar-orbiting meteorological satellites for the intersatellite calibration of radiometers. Journal of Atmospheric and Oceanic Technology, 21: 537–542

Cao C, Xiong X, Wu A, Wu X (2008). Assessing the consistency of AVHRR and MODIS L1B reflectance for generating Fundamental Climate Data Records. J Geophys Res, 113, D09114. doi: 10.1029/2007JD009363

Cao C, Xu H, Sullivan J, McMillin L, Ciren P, Hou Y (2005). Intersatellite radiance biases for the High Resolution Infrared Radiation Sounders (HIRS) onboard NOAA-15, -16, and -17 from simultaneous nadir observations. Journal of Atmospheric and Oceanic Technology, 22(4): 381–395

Chander G, Xiong X, Angal A, Choi T (2009). An Assessment of African Test Sites in the Context of a Global Network of Quality-Assured Reference Standards. Proceedings of IGARSS 2009

Cohen W B, Goward S N (2004). Landsat's role in ecological applications of remote sensing. BioScience, 54 (6): 535–545

Eplee R E, Bailey S, Barnes R, Kieffer H H, McClain C R (2006). Comparison of SeaWiFS on-orbit Lunar and Vicarious Calibrations. Proceedings of SPIE 6296

Esaias W, Abbott M, Barton I, Brown O, Campbell J, Carder K, Clark D, Evans R, Hoge F, Gordon H, Balch W, Letelier R, Minnett P (1998). An Overview of MODIS Capabilities for Ocean Science Observations. IEEE Trans Geosci Remote Sensing, 36: 1250–1265

Goward S N, Irons J, Franks S, Arvidson T, Williams D, Faundeen J (2006). Historical record of landsat global coverage: mission operations, NSLRSDA, and international cooperator stations. Photogrammetric Engineering and Remote Sensing, 72: 1155–1169

Goward S N, Williams D L (1997). Landsat and Earth Systems Science: development of terrestrial monitoring. Photogrammetric Engineering and Remote Sensing, 63 (7): 887–900

Guenther B, Butler J, Ardanuy P (1997). Workshop on Strategies for Calibration and Validation of Global Change and Measurements. NASA Reference Publication1397

Heidinger A K, Cao C, Sullivan J T (2002). Using Moderate Resolution Imaging Spectrometer (MODIS) to calibrate advanced very high resolution radiometer reflectance channels, J Geophys Res, 107 (D23), 4702. doi: 10.1029/2001JD002035

Hook S, Vaughan R, Tonooka H, Schladow S (2007). Absolute Radiometric In-Flight Validation of Mid and Thermal Infrared Data from ASTER and MODIS on the Terra Spacecraft Using the Lake Tahoe CA/NV, USA Automated Validation Site. IEEE Trans Geosci Remote Sensing, 45(6): 1798–1807

Justice C, Vermote E, Townshend J, Defries R, Roy D, Hall D, Salomonson V, Privette J, Riggs G, Strahler A, Lucht W, Myneni B, Lewis P, Barnsley M (1998). The Moderate Resolution Imaging Spectroradiometer (MODIS): land Remote Sensing for Global Change Research. IEEE Trans Geosci Remote Sensing, 36: 1228–1249

Kieffer H H, Stone T (2005). The Spectral Irradiance of the Moon. The Astron J, 129(6): 2887–2901

King M, Menzel W, Kaufman Y, Tanre D, Gao B, Platnick S, Ackerman S, Remer L, Pincus R, Hubanks P (2003). Cloud and aerosol properties, precipitable water, and profiles of temperature and water vapor from MODIS. IEEE Trans Geosci Remote Sensing, 41: 442–458

Markham B, Thome K, Barsi J, Kaita E, Helder D, Barker J, Scaramuzza, P (2004). Landsat-7 ETM+ on-orbit reflective-band radiometric stability and absolute calibration. IEEE Trans Geosci Remote Sensing, 42(12): 2810–2820

Masek J G, Vermote E, Huang C, Wolfe R, Cohen W, Hall F, Kutler J, Nelson P (2008). North American forest disturbance mapped from a decadal Landsat record. Remote Sensing of Environment, 112: 2914–2926

Minnett P, Brown O, Evans R, Key E, Kearns E, Kilpatrick K, Kumar A, Maillet K, Szczodrak M (2004). Sea-surface Temperature Measurements from the Moderate-Resolution Imaging Spectroradiometer (MODIS) on Aqua and Terra. Proceedings of IGARSS2004: 4576–4579

Ohring B, Wielicki R, Spencer B, Emery W, Datla R (2004). Workshop Report: Satellite Instrument Calibration for Measuring Global Climate Change. NISTIR 7074

Ohring G, Anderson J G, Ardanuy P, Bingham G, Butler J, Cao C, Datla R, Dykema J, Emery W, Flynn L, Fraser G, Goldberg M, Kopp G, Iguchi T, Kunkee D, Leroy S, Miller L, Pollock D, Revercomb H, Shipley S, St. Germain K, Stone T, Tansock J, Thurgood A, Tobin D, Ungar S, Weng F, Wielicki B, Winker D, Xiong X (2008). Achieving Satellite Instrument Calibration for Climate Change. Camp Spring: NOAA NESDIS Publication

Parkinson C L (2003). Aqua: an earth-observing satellite mission to examine water and other climate variables. IEEE Trans Geosci Remote Sensing, 41: 173–183

Rao N, Chen J (1999). Revised post-launch calibration of the visible and near-IR channels NOAA14/AVHRR. Int J Remote Sens, 20: 3485–3491

Salomonson V, Barnes W, Xiong X, Kempler S, Masuoka E (2002). An Overview of the Earth Observing System MODIS Instrument and Associated Data Systems Performance. Proceedings of IGARSS, 2002

Schaaf C B, Gao F, Strahler A H, Lucht W, Li X, Tsang T, Strugnell N C, Zhang X, Jin Y, Muller J P, Lewis P, Barnsley M, Hobson P, Disney M, Roberts G, Dunderdale M, Doll C, d'Entremont R P, Hu N, Liang S, Privette J L, Roy D (2002). First operational BRDF, albedo nadir reflectance products from MODIS. Remote Sensing of Environment, 83: 135–148

Six D, Fily M, Alvain S, Henry P, Benoist J (2004). Surface Characterisation of the Dome Concordia Area (Antarctica) as a Potential Satellite Calibration Site Using SPOT 4/VEGETATION Instrument. Remote Sensing of Environment, 89: 83–94

Steyn-Ross D A, Steyn-Ross M, Clift S (1992). Radiance calibrations for AVHRR infrared channels. J Geophys Res, 97 (C4): 5551–5568

Sun J, Xiong X, Barnes W L, Guenther B (2007). MODIS reflective solar bands on-orbit lunar calibration. IEEE Trans Geosci Remote Sens, 45(7): 2383–2393

Thome K, Czapla-Myer J, Biggar S (2003). Vicarious calibration of Aqua and Terra MODIS. In: Proceedings of SPIE 5151: 395–405

Trishchenko A P (2002). Removing unwanted fluctuations in the AVHRR thermal calibration data using robust techniques. Journal of Atmospheric and Oceanic Technology, 19: 1939–1954

Trishchenko A P, Fedosejevs G, Li Z, Cihlar J (2002). Trends and uncertainties in thermal calibration of AVHRR radiometers onboard NOAA-9 to NOAA-16. J Geophys Res, 107 (24): 1701–1713

Vogelmann J E, Howard S M, Yang L, Larson C R, Wylie B K, Van Driel J N (2001). Completion of the 1990's National Land Cover Data Set for the conterminous United States. Photogrammetric Engineering and Remote Sensing, 67: 650–662

Walton C, Sullivan J, Rao C, Weinreb M (1998). Corrections for detector nonlinearities and calibration inconsistencies of the infrared channels of the AVHRR. J Geophys Res, 103: 3323–3337

Wan Z, Zhang Y, Zhang Q, Li Z (2004). Quality Assessment and Validation of the MODIS Global Land Surface Temperature. Int J Remote Sensing, 25(1): 261–274

Warren S G, Brandt R E (1998). Effect of surface roughness on bidirectional reflectance of Antarctic snow. J Geophys Res, 103, E11, 25: 789–807

Wenny B, Xiong X (2008). Using a Cold Earth Surface Target to Characterize Long-term Stability of the MODIS Thermal Emissive Bands. IEEE Geosci Remote Sens Let, 5(2): 162–165

Woodcock C E, Macomber S A, Pax-Lenney M, Cohen W C (2001). Monitoring large areas for forest change using Landsat: Generalization across space, time and Landsat sensors. Remote Sensing of Environment, 78: 194–203

Wu A, Cao C, Xiong X (2003). Intercomparison of the 11-and 12-μm bands of Terra and Aqua MODIS using NOAA-17 AVHRR. Proceedings of SPIE 5151: 384–394

Wu A, X Xiong X, Cao C (2008). Terra and Aqua MODIS Intercomparison of three reflective solar bands using AVHRR onboard the NOAA-KLM satellites. Int J Remote Sens, 29(7): 1997–2010

Wulder M A, White J C, Goward S N, Masek J G, Irons J R, Herold M, Cohen W B, Loveland T R, Woodcock C E (2008). Landsat continuity: issues and opportunities for land cover monitoring. Remote Sensing of Environment, 112: 955–969

Xiong X, Barnes W (2006). An Overview of MODIS radiometric calibration and characterization. Advances in Atmospheric Sciences, 23(1): 69–79

Xiong X, Chiang K, Esposito J, Guenther B, Barnes W (2003). MODIS on-orbit calibration and characterization. motrologia, 40: 89–92

Xiong X, Sun J, Barnes W (2008). Inter-comparison of on-orbit calibration consistency between terra and aqua MODIS reflective solar bands using the moon. IEEE Geosci Remote Sens Let, 5(4): 778–782. doi: 10.1109/LGRS.2008.2005591

Xiong X, Wenny B, Barnes W L (2009a). Overview of NASA earth observing systems terra and aqua moderate resolution imaging spectroradiometer instrument calibration algorithms and on-orbit performance. J Appl Remote Sens, 3, 032501. doi: 10.1117/1.3180864

Xiong X, Wu A, Cao C (2008). On-orbit calibration and intercomparison of terra and aqua MODIS surface temperature spectral bands, Int J Remote Sens, 29(17): 5347–5359

Xiong X, Wu A, Sun J, Wenny B (2006). An overview of intercomparison methodologies for terra and aqua MODIS calibration. Proceedings of SPIE 6296, 62960C. doi: 10.1117/12.679162

Xiong X, Wu A, Wenny B (2009b). Using dome C for MODIS calibration stability and consistency. J Appl Remote Sens, 3, 033520, doi: 10.1117/1.3116663